Geophysical Research Letters

RESEARCH LETTER
10.1029/2022GL101900

Key Points:

- A close relationship is found between serial cyclone clustering (SCC) at 5°W and weather regimes (WRs) in the North Atlantic-European region
- SCC in mid and high latitudes (55°N, 65°N) is mainly associated with cyclonic and in low latitudes (45°N) with anticyclonic WR life cycles
- Regardless of the selected latitude, SCC occurs mostly during an active regime life cycle and is manifested in a well-established WR

Supporting Information:

Supporting Information may be found in the online version of this article.

Correspondence to:

S. Hauser,
seraphine.hauser@kit.edu

Citation:

Hauser, S., Mueller, S., Chen, X., Chen, T.-C., Pinto, J. G., & Grams, C. M. (2023). The linkage of serial cyclone clustering in Western Europe and weather regimes in the North Atlantic-European region in boreal winter. *Geophysical Research Letters*, *50*, e2022GL101900. https://doi.org/10.1029/2022GL101900

Received 2 NOV 2022
Accepted 26 DEC 2022

Author Contributions:

Conceptualization: Joaquim G. Pinto, Christian M. Grams
Data curation: Seraphine Hauser, Sebastian Mueller, Xiaoyang Chen, Ting-Chen Chen, Joaquim G. Pinto, Christian M. Grams
Formal analysis: Seraphine Hauser, Sebastian Mueller, Xiaoyang Chen, Ting-Chen Chen, Joaquim G. Pinto, Christian M. Grams
Funding acquisition: Joaquim G. Pinto, Christian M. Grams

The Linkage of Serial Cyclone Clustering in Western Europe and Weather Regimes in the North Atlantic-European Region in Boreal Winter

Seraphine Hauser[1], Sebastian Mueller[1], Xiaoyang Chen[1], Ting-Chen Chen[1], Joaquim G. Pinto[1], and Christian M. Grams[1]

[1]Department Troposphere Research (IMK-TRO), Institute of Meteorology and Climate Research, Karlsruhe Institute of Technology (KIT), Karlsruhe, Germany

Abstract Extra-tropical cyclones are an important source of weather variability in the mid-latitudes. Multiple occurrences in a short period of time at a particular location are denominated serial cyclone clustering (SCC), and potentially lead to large societal impacts. We investigate the relationship between SCC affecting Western Europe and large-scale weather regimes (WRs) in the North Atlantic-European region in boreal winter. We find that SCC in low latitudes (45°N) is predominantly associated with the anticyclonic Greenland Blocking WR. In contrast, SCC in mid and high latitudes (55°N, 65°N) is mostly linked to different cyclonic WRs. Thereby, SCC occurs typically within a well-established WR that builds up prior to SCC and decays after SCC. Thus, SCC events are closely associated with recurrent, quasi-stationary and persistent large-scale flow patterns (WRs). This mutual relationship reveals the potential of WRs in forecasting storm series and associated impacts on sub-seasonal to seasonal time scales.

Plain Language Summary Serial cyclone clustering describes the occurrence of multiple extra-tropical cyclones within a certain time frame and a spatially restricted region. Since extra-tropical cyclones can be associated with strong winds and heavy precipitation, multiple occurrences can lead to large cumulative impacts in the affected areas. We analyze the relationship between serial cyclone clustering (SCC) in Western Europe and so-called weather regimes (WRs) in the North Atlantic-European region in boreal winter. These regimes describe slow evolving and enduring large-scale atmospheric circulation patterns. Relationships with certain regime types are identified but depend on the latitude at which the clustered frequency of extra-tropical cyclones is found. When SCC occurs in low latitudes (45°N), it mostly appears coincident with anticyclonic large-scale flow patterns. In contrast, SCC in mid and high latitudes (55°N, 65°N) often occurs simultaneously with different cyclonic regimes. We find that periods of SCC occur typically within WR life cycles pointing to the fact that both, the WRs and SCC periods, are interlinked. This relationship may facilitate forecasting storm series and associated impacts on time scales beyond 2 weeks.

1. Introduction

Extra-tropical cyclones are a common feature of the North Atlantic-European region (NAE), determining both day-to-day weather variability as well as the average climatic conditions. Extreme extra-tropical cyclones can lead to wind gusts, widespread precipitation, and sometimes storm surges (e.g., Dangendorf et al., 2016; Fink et al., 2009). Frequently, such storms do not appear as single events. One recent example was the subsequent occurrence of storms Dudley, Eunice, and Franklin as named by United Kingdom's national weather service in mid-February 2022, which led to considerable damage and disruption across Western Europe (e.g., Mühr et al., 2022). Other prominent periods include February 1990, January 1993, December 1999, January 2007, and February 2014 (Matthews et al., 2014; Pinto et al., 2014). The seminal work of Bjerknes and Solberg (1922) had already recognized that multiple cyclones may develop along a frontal system, and denominated this phenomena as "cyclone families." Modern nomenclature refers to serial (temporal) cyclone clustering (Dacre & Pinto, 2020; Mailier et al., 2006; Vitolo et al., 2009) or to temporally compounding events (e.g., Bevacqua et al., 2021; Zscheischler et al., 2020). Such a group of events affects a region within a short period of time and can lead to cumulative impacts. Hereafter we use the term serial cyclone clustering (SCC) for this phenomenon. In their review paper, Dacre and Pinto (2020) pointed out two main physical reasons for the occurrence of SCC that are not necessarily independent and could occur at the same time: (a) the steering through the large-scale atmospheric

Investigation: Seraphine Hauser, Sebastian Mueller, Xiaoyang Chen, Ting-Chen Chen
Methodology: Seraphine Hauser, Sebastian Mueller, Xiaoyang Chen, Ting-Chen Chen, Joaquim G. Pinto, Christian M. Grams
Project Administration: Seraphine Hauser, Joaquim G. Pinto, Christian M. Grams
Resources: Seraphine Hauser, Xiaoyang Chen, Ting-Chen Chen, Joaquim G. Pinto, Christian M. Grams
Software: Seraphine Hauser, Sebastian Mueller, Xiaoyang Chen, Ting-Chen Chen
Supervision: Seraphine Hauser, Joaquim G. Pinto, Christian M. Grams
Validation: Seraphine Hauser, Sebastian Mueller, Xiaoyang Chen, Ting-Chen Chen
Visualization: Seraphine Hauser, Sebastian Mueller
Writing – original draft: Seraphine Hauser, Xiaoyang Chen, Joaquim G. Pinto, Christian M. Grams
Writing – review & editing: Seraphine Hauser, Ting-Chen Chen, Joaquim G. Pinto, Christian M. Grams

flow, typically characterized by an intensified, quasi-stationary jet-stream extending from the Central North Atlantic toward Western Europe for several days (e.g., Messori & Caballero, 2015; Pinto et al., 2014), and (b) secondary cyclogenesis on the trailing cold front of a pre-existing cyclone (e.g., Parker, 1998; Pinto et al., 2014; Weijenborg & Spengler, 2020).

The large-scale atmospheric circulation over the NAE can be characterized in terms of a comparatively small number of states, often referred to as "weather regimes," "Grosswetterlagen," or phases of a teleconnection pattern (e.g., North Atlantic Oscillation (NAO)) (Wanner et al., 2001). Weather regimes (hereafter WRs) are recurrent, quasi-stationary, and persistent large-scale atmospheric circulation states (Hannachi et al., 2017). In the late 1940s, weather forecasters recognized their importance (e.g., Levick, 1949) and Charney and DeVore (1979) hypothesized that the large-scale atmospheric circulation moves between these multiple equilibrium states. It is debated whether WRs are a mere statistical characterization or if they have a deeper physical foundation. Evidence in favor of the latter has recently been provided by Faranda et al. (2016, 2017), and Hochman et al. (2021). Given that WRs characterize the slower variability of the large-scale atmospheric conditions over the region and can establish conditions favorable for large-scale extremes (Beerli & Grams, 2019; Lavaysse et al., 2018; Pasquier et al., 2019; Yiou & Nogaj, 2004), their assessment and consideration is important for medium-range, and sub-seasonal to seasonal (S2S) weather prediction and climate projections (Merryfield et al., 2020; Santos et al., 2016; White et al., 2021). WRs in the NAE are mostly derived based on geopotential height, although the season considered and the statistical approaches used to define them may differ. This leads to the fact that the number of regimes can vary between 2 and 7 (Falkena et al., 2020). The transitions between WRs are often associated with Rossby wave breaking (e.g., Michel & Rivière, 2011).

The question arises if a clear relationship between the occurrence of SCC at a certain location and the occurrence of specific WRs exists. For example, Priestley et al. (2017a) noted the differences on the large-scale atmospheric conditions associated with the occurrence of SCC at 45°N, 55°N, and 65°N along the 5°W longitude. In high latitudes (65°N), the intensified and extended jet-stream was constrained by Rossby wave breaking on both sides of the jet but the cyclonic wave breaking to the north was dominant for SCC near the British Isles (55°N). In lower latitudes (45°N), the anticyclonic wave breaking was absent, leading to an almost zonal jet-stream (Priestley et al., 2017a). In this study, we use an extended definition of seven North Atlantic-European WRs (Grams et al., 2017) to investigate the link between the occurrence of SCC in Western Europe and WRs in boreal winter (December-January-February (DJF)). The study is organized as follows. First, we investigate the relationship between SCC and WRs along two contrasting winter periods to showcase the potential role of SCC (Section 3.1). Second, we present the modulated occurrence frequency of WRs around SCC events (Section 3.2). Finally, we examine the timing of SCC and WRs (Section 3.3) and to answer the question: Is the WR preceding SCC or is SCC preceding the WR?

2. Data and Methodology

Our study is based on the ERA-Interim reanalysis (Dee et al., 2011) of the European Centre for Medium-Range Weather Forecasts (ECMWF) for January 1979–August 2019, remapped from the native resolution of T255 to a regular latitude-longitude grid with $1 \times 1°$ and a temporal resolution of 6 hr.

2.1. Cyclone Tracking and Serial Cyclone Clustering

To identify extratropical cyclone tracks, we apply a cyclone tracking algorithm (Murray & Simmonds, 1991; Pinto et al., 2005) to the mean sea level pressure (p) fields of ERA-Interim. The algorithm is run for the region 20°N–90°N and for the entire ERA-Interim data period. The algorithm primarily searches for the minimum p in the vicinity of a $\nabla^2 p$ maximum as cyclone centers. To filter out weak and thermal lows, we follow Pinto et al. (2009) to retain cyclones only if they fulfill the following criteria: (a) cyclone lifetime ≥24 hr, (b) life-time maximum $\nabla^2 p > 0.6$ hPa degree latitude^{-2}, and (c) maximum $\frac{\mathrm{d}}{\mathrm{d}t} \nabla^2 p \geq 0.3$ hPa degree latitude^{-2} d^{-1} for a 24-hr period. Systems located above a terrain height of 1,500 m are removed to avoid artifacts introduced by the extrapolation of p below ground.

For the identification of SCC, we use an absolute frequency metric following Pinto et al. (2014) and Priestley et al. (2017b). To account for SCC at different latitudes, three base areas covered by a 700 km radius around different points in Western Europe (65°N/5°W, 55°N/5°W, 45°N/5°W) are considered. As we wish to target

"strong" cyclones with respect to the local climatology, intensity thresholds are defined locally at the three latitude-longitude grid points, based on their 5th percentile of the respective p climatology during winter (DJF, 1979–2019). The obtained thresholds are 972.5, 983.2, and 999.1 hPa at 65°N, 55°N, and 45°N, respectively. For each region, a passing cyclone is counted on the day when it reaches a relative peak intensity (minimum p) within the area and only if such minimum p is lower than the respective 5th percentile threshold. Finally, time series of daily number of cyclones are obtained for the period November–March from 1979/1980 to 2018/2019.

A day d is considered clustered if the running sum of the cyclones passing the area over 7 days (±3 days around d) is greater than or equal to 4 for SCC at 55°N and 65°N. For SCC at 45°N, this running sum is set down to 3 as fewer and weaker cyclones occur in lower latitudes in winter (Neu et al., 2013). Preliminary SCC periods are defined by adding ±3 days around each clustering day. To investigate the link to WR life cycles, the definition of the begin of a SCC period is essential. Therefore, the following conditions determine the final SCC periods: (a) the preliminary SCC periods are adjusted so that the first day (onset) is associated with the first occurrence of at least one cyclone in the series of cyclones (same applies for the SCC decay as the last day in the SCC period with at least one cyclone), (b) SCC periods are allowed to start in November or end in March but must overlap with DJF for at least 1 day, and (c) SCC periods must have a minimum length of 2 days. For the 40 winter periods considered here, we identify 54 periods for SCC at 65°N, 43 periods for SCC at 55°N, and 36 periods for SCC at 45°N. Various characteristics of the SCC periods at different latitudes are listed in Supporting Information S1 (Table S1, Figure S2).

2.2. Weather Regimes in the North Atlantic-European Region

The ERA-Interim data set from 1979 to 2015 is used to retrieve year-round WRs in the North Atlantic-European region (NAE; 80°W–40°E, 30°N–90°N) following the method of Grams et al. (2017). We use geopotential height anomalies at 500 hPa (Z500') every 6 hr based on a 90-day running mean climatology (1979–2015) and apply a 10-day low-pass filter to exclude high-frequency signals. Since we aim for a year-round definition, we normalize the anomalies. To do so, the temporal standard deviation of Z500' is computed for each calendar time i in the time period ±15 days around i for all years (1979–2015) at each grid point. We then define a normalization weight for each calendar time as the spatial average in the NAE domain of this running standard deviation. This definition of year-round WRs represents a refinement of the original algorithm of Grams et al. (2017). We here apply a latitudinal weighting when computing the spatial average for the normalization weights, which improves the detection of regimes in summer and slightly reduces the number of days attributed to a regime in winter (now 74.7% vs. originally 77.0% for DJF in 1979–2015). The time series of the normalization weight shows a maximum in the winter months and a minimum in the summer months (not shown). After the normalization, a k-means clustering is performed for the expanded phase space of the leading seven empirical orthogonal functions that explain 74.8% of the variability (see Grams et al., 2017, for details). The resulting 7 WRs (Figure S1 in Supporting Information S1) consist of 3 cyclonic regime types (Atlantic Trough (AT); Zonal regime (ZO); Scandinavian Trough (ScTr)) and 4 anticyclonic regime types (Atlantic Ridge (AR); European Blocking (EuBL); Scandinavian Blocking (ScBL); Greenland Blocking (GL)). Within these regimes, ZO represents the positive and GL the negative phase of the NAO.

We compute a WR index (I_{WR}) following Michel and Rivière (2011), applied to low-pass filtered Z500', to quantitatively describe active WRs (Grams et al., 2017). The I_{WR} represents the normalized projection of low-pass filtered Z500' onto the mean low-frequency Z500' WR pattern and is computed at each time for all 7 WRs. Objective WR life cycles are derived based on the I_{WR} for all WRs. A WR life cycle is detected if $I_{WR} > 1.0$ for more than 5 consecutive days following an earlier definition of Michel and Rivière (2011). Within the WR life cycle, the I_{WR} has to be larger than any other I_{WR} for at least one time step. Analogous to the SCC periods, the first time when $I_{WR} > 1.0$ serves as WR life cycle onset time and the last day when $I_{WR} > 1.0$ as decay time. Since several WR life cycles can be active at the same time, we determine the dominant WR type as the active WR with the highest projection, that is, the highest I_{WR}. If no WR life cycle is active, the large-scale flow at that time cannot be classified into one of the 7 WRs and falls into the no regime category (26.6% of all times during DJF 1979–2019). Even though the WRs are defined based on the 1979–2015 data period, the I_{WR} and WR life cycles can also be computed beyond this data period. In this study, we perform these calculations for the period 1979–2019.

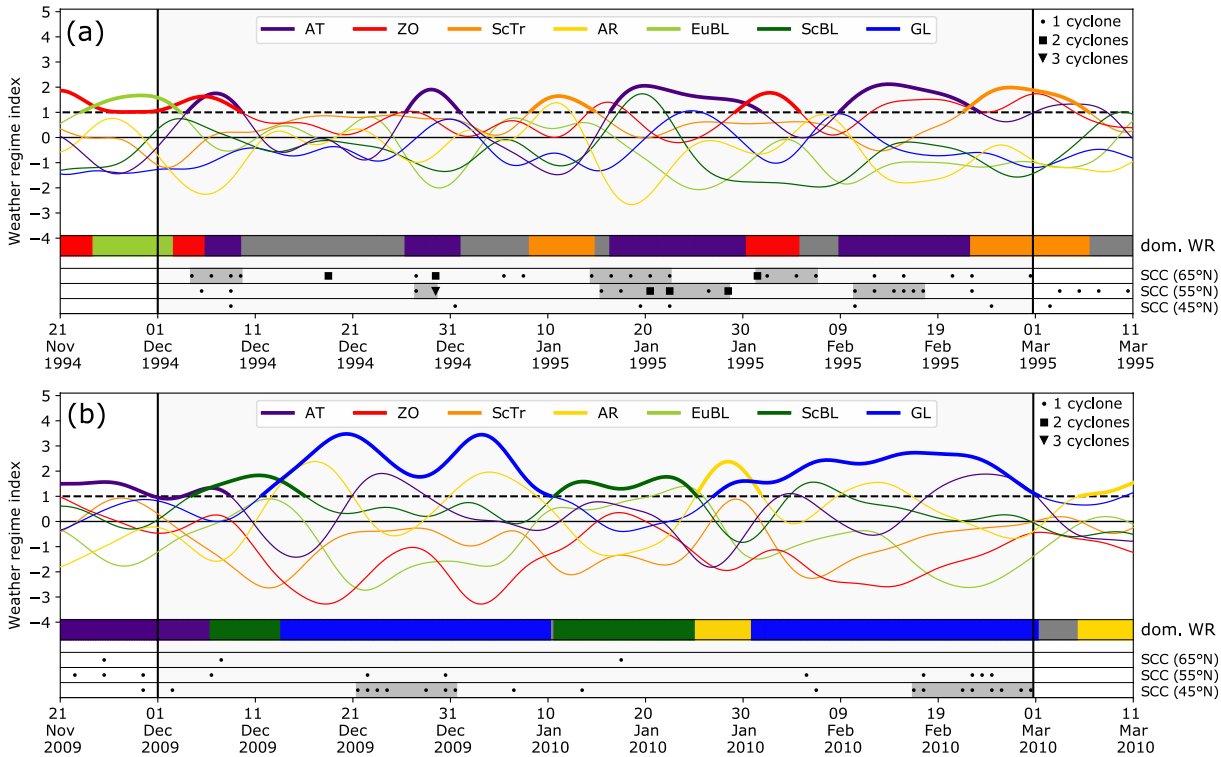

Figure 1. Time series of I_{WR} for North Atlantic-European weather regimes (WRs) and serial cyclone clustering (SCC) periods in winter (a) 1994/1995 and (b) 2009/2010. Colored lines represent I_{WR} for each of the 7 WRs: the 3 cyclonic regimes Atlantic Trough (AT), Zonal regime (ZO), and Scandinavian Trough (ScTr), and the 4 anticyclonic regimes, Atlantic Ridge (AR), European Blocking (EuBL), Scandinavian Blocking (ScBL), and Greenland Blocking (GL). Thick colored lines point to an active regime life cycle. Dominant WR for each time step is highlighted in the respective WR color in uppermost horizontal bar with times without active WR life cycle marked gray. SCC periods for the three different latitudes (65°N, 55°N, and 45°N) marked in gray in the three horizontal bars below. The different black markers in the horizontal bars show the number of passing cyclones for the considered SCC (per day).

3. Results

3.1. Two Contrasting Winters as Case Studies

We first illustrate the occurrence of SCC in Western Europe and WRs over the NAE with case studies. From the 40 available winter periods, we contrast two winters which had adverse weather impacts in Europe (Figure 1): winter 1994/1995 which was characterized by wet conditions in Central Europe (Dunstone et al., 2018), and winter 2009/2010 which was associated with several cold spells in Western and Northern Europe (Cattiaux et al., 2010).

The large-scale atmospheric flow during winter 1994/1995 was almost exclusively dominated by cyclonic WRs in the NAE, especially by AT (Figure 1a). Often active WR life cycles did not directly transition from one to another and thus were preceded or followed by a large-scale pattern not corresponding to the 7 WRs (no regime). During winter 1994/1995, SCC occurred exclusively in mid and high latitudes (55°N, 65°N) and during cyclonic WRs. Interestingly, SCC at 55°N occurred exclusively during the AT regime in winter 1994/95. However, SCC was additionally linked to ZO and slightly to ScTr in high latitudes (65°N).

Compared to winter 1994/1995, anticyclonic WR life cycles dominated over the NAE in winter 2009/2010 (Figure 1b). Interestingly, almost every day in this winter was characterized by a persistent WR. SCC in winter 2009/2010 occurred exclusively in low latitudes (45°N) and the associated SCC periods were longer compared to the mid and high latitude SCC periods in winter 1994/1995 (Figure 1). Both SCC periods identified at 45°N were associated with the GL regime, which was dominant for more than half of the winter time. In fact, the winter 2009/2010 was characterized by a very anomalous and long-lasting negative NAO phase (Osborn, 2011). In both cases, it is striking that the GL regime built up well before the start of the SCC periods.

The comparison of the occurrence of different WRs and SCC for two contrasting winters provides evidence that SCC in mid and high latitudes may be associated with cyclonic rather than anticyclonic WRs (winter 1994/1995,

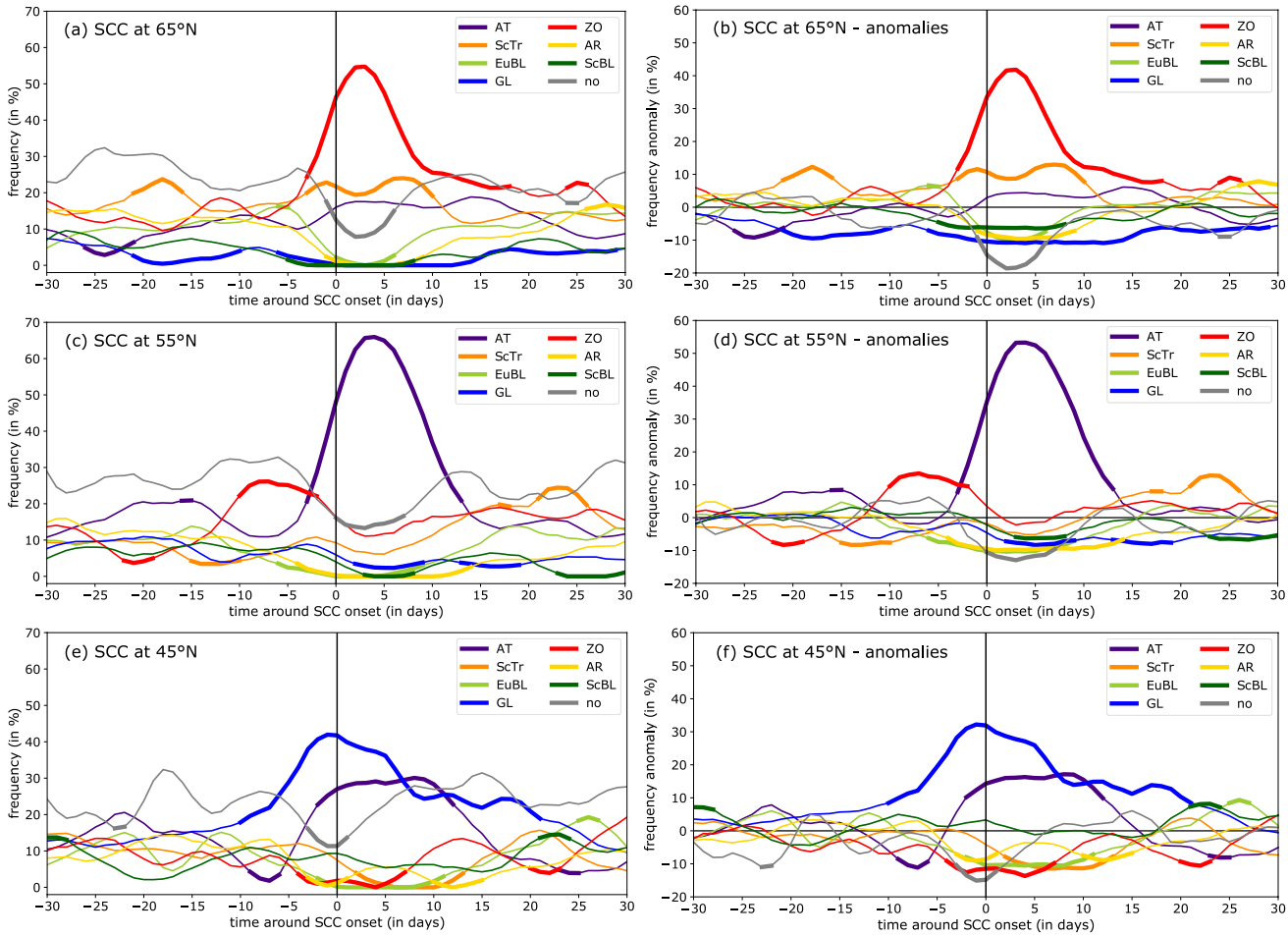

Figure 2. Daily lagged weather regime (WR) frequencies and frequency anomalies centered around serial cyclone clustering (SCC) onsets at 65°N, 55°N, and 45°N. Colored lines represent frequency (a, c, e) and frequency anomaly (b, d, f) of each WR (Atlantic Trough (AT), Scandinavian Trough (ScTr), Zonal regime (ZO), Atlantic Ridge (AR), European Blocking (EuBL), Scandinavian Blocking (ScBL), Greenland Blocking (GL)) and no regime (no) that is dominant at a certain lag relative to the SCC onset. Thick lines mark statistically significant values based on the percentile ranking with $\alpha = 0.05$. See Text S1 in Supporting Information S1 for details on the anomaly calculation and significance test.

Figure 1a). The results for winter 2009/2010 suggest that SCC in low latitudes over Western Europe is associated with anticyclonic regime types (Figure 1b). In the next Subsection we will investigate whether this finding holds when considering all winter periods from 1979 to 2019.

3.2. Weather Regime Frequency Around Serial Cyclone Clustering Periods

In order to understand the relationship between SCC and WRs, we here perform a lagged WR frequency analysis based on the definition of the dominant WR type around all SCC onsets in winter (Figure 2). Additionally, we compute WR frequency anomalies and assess statistical significance following Domeisen et al. (2020) (see documentation in Supporting Information S1 (Text S1)). Figure S3 in Supporting Information S1 provides a related analysis based on the I_{WR}. Maps of cyclone track density during SCC and each WR can be found in Supporting Information S1 (Figures S4 and S5).

SCC in high latitudes (65°N) co-occurs with a significantly increased frequency of almost exclusively cyclonic WRs (AT, ZO, ScTr) from SCC onset and up to 2 weeks thereafter (Figures 2a and 2b). ZO is identified as the dominant WR from shortly prior to the SCC onset until 18 days after SCC onset. More than 50% of all considered SCC periods at 65°N are associated with ZO. The increased frequency of ZO reaches a maximum of 55% around 3 days after onset which reflects a quadrupling of the climatological frequency of ZO in DJF. The frequency of ScTr regime is also increased and doubled compared to climatology but only up to 10 days after SCC. The

patterns of cyclone track density for ZO, ScTr, and SCC at 65°N with a maximum in density near Iceland agree well, corroborating the systematic linkage of SCC at 65°N to these regimes (Figures S4a and S5b in Supporting Information S1). AT also occurs more frequently, though the signal is not significant (Figures 2a and 2b). The frequency of anticyclonic WRs is significantly diminished shortly prior to SCC onset and up to 3 weeks thereafter (Figure 2b). In particular, during the first few days after SCC onset, none of the SCC periods at 65°N is dominated by an anticyclonic regime (Figure 2a). EuBL is the only anticyclonic regime with significantly above normal frequency at about 5 days before onset, but this signal vanishes rapidly before SCC onset. Cyclone activity during anticyclonic WRs is weak in the clustering areas and occurs significantly upstream or far north. Therefore, anticyclonic WR are not related to cyclone activity during SCC at 65°N (Figures S5d–S5g in Supporting Information S1).

Cyclonic regimes also dominate the large-scale circulation around SCC periods at 55°N (Figures 2c and 2d). However, the dominant cyclonic regime here is AT, which co-occurs with SCC in more than 65% of all SCC periods. Patterns of cyclone track density show a high agreement between AT and SCC at 55°N with a maximum west of the British Isles (Figures S4b and S5a in Supporting Information S1). An increased frequency of AT is found from −3 to about 15 days around SCC onset and represents more than a five-fold increase of frequency compared to climatology around 5 days after SCC onset. ZO occurs frequently before SCC periods, but the significant frequency anomaly decreases with the onset of SCC which raises the question whether a transition from ZO to AT may help to set the large-scale conditions for SCC to occur. The frequency of anticyclonic regimes is significantly decreased during SCC periods at 55°N (Figures 2c and 2d).

SCC at low latitudes (45°N) goes along with a strong increase in the frequency of the anticyclonic GL regime (Figures 2e and 2f), which corresponds to a negative NAO phase. The strongest and significant signals are identified from −10 days to over +20 days around SCC onset. In contrast to the cyclonic regimes dominating SCC in mid and high latitudes, the maximum frequency increase occurs shortly prior to SCC onset with a maximum frequency of around 42%, which corresponds to a four-fold increase of the GL frequency. A zonally elongated cyclone track density is visible in lower latitudes over Europe for GL and indicates the link to SCC at 45°N (Figures S4c and S5g in Supporting Information S1). In addition to GL, AT occurs anomalously often during SCC at 45°N (Figures 2e and 2f). The increased frequency of AT represents more than a doubling of the climatological frequency. We observe a rapid increase of the AT frequency in the 5 days prior to SCC onset suggesting a regime transition. However, the increased significant frequency of AT develops later (−3 days prior to SCC onset) and ends earlier (12 days after SCC onset) than the dominating increased frequency of GL, which suggests case-to-case variability.

In summary, we find significant changes in the large-scale circulation pattern prior to SCC onsets regardless of the latitude over Western Europe at which SCC occurs. The climatological results agree well with the observations in the exemplary case study of the winters 1994/1995 and 2009/2010 (Figure 1): SCC in low latitudes (45°N) is predominantly associated with the anticyclonic GL WR, and SCC in mid and high latitudes mostly occurs simultaneously with cyclonic WRs. An interesting observation is the significantly lowered frequency of the no regime, that is, when the large-scale flow field cannot be assigned to one of the 7 WRs. Thus, the occurrence of SCC is associated with the occurrence of recurrent, quasi-stationary, and persistent large-scale flow patterns rather than an unusual large-scale flow pattern. In a last step, we will now consider whether SCC triggers a particular WR or whether a WR sets up the large-scale conditions for an SCC event.

3.3. The Mutual Linkage of Serial Cyclone Clustering and Weather Regimes

The two different winter periods 1994/1995 and 2009/2010 (Figure 1) demonstrate that different WR life cycles may be active simultaneously or there may be a transition between WR life cycles during a SCC period. Indeed, we find that 68.5% (65°N), 55.2% (55°N), and 44.5% (45°N) of all SCC periods are associated with more than one WR life cycle. Therefore, we take into account all WR life cycles that overlap with SCC periods in the following. We now determine the time difference between WR life cycle and SCC onset, and between WR life cycle and SCC decay to understand what evolved first: a clustered occurrence of synoptic-scale extra-tropical cyclones or the establishment of a specific large-scale flow pattern. Analogously, the question arises whether a WR pattern that has built up changes again before or after the occurrence of SCC (Figure 3).

SCC at 65°N is predominantly associated with cyclonic WR life cycles that start before the SCC onset and end after SCC decay (Figure 3a). The large spatial overlap of the confidential ellipses shows that this statement applies

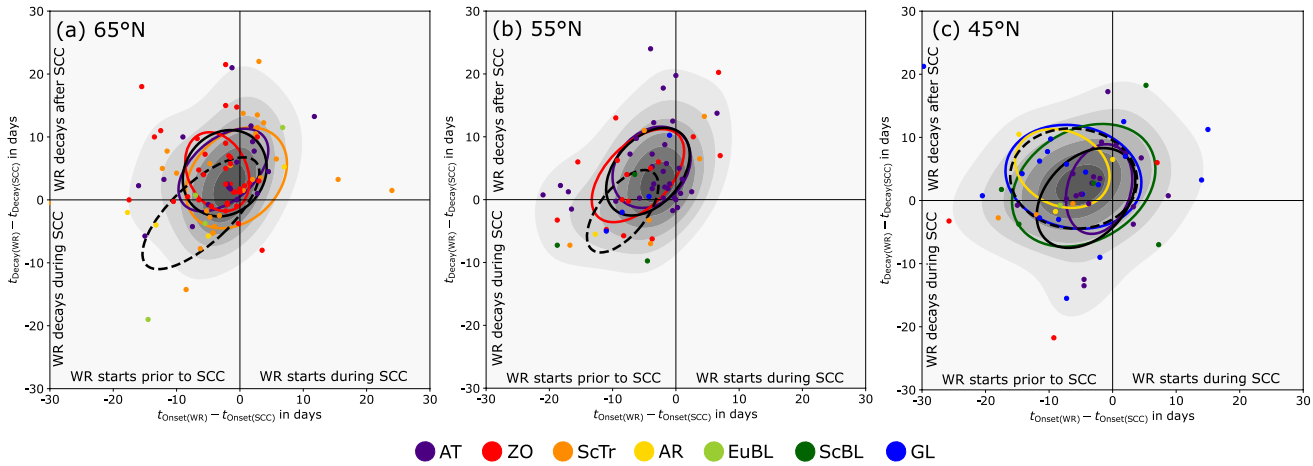

Figure 3. Time offset of serial cyclone clustering (SCC) life cycle and associated weather regime (WR) life cycle for (a) 65°N, (b) 55°N, and (c) 45°N. Scatter plot of time offset between WR onset and SCC onset (abscissa) and WR decay and SCC decay (ordinate) in colored points (colors according to regime type). All active regime life cycles that overlap with a SCC period are considered here. Point density via kernel density estimation is shown in gray shading (normalized, from 0.0 to 1.05 in steps of 0.15). Confidential ellipses are drawn for selected WRs with radius limited to one standard deviation. In addition, confidential ellipses are shown for all anticyclonic WRs (dashed black) and cyclonic WRs (solid black).

to all cyclonic WR types with the strongest signal in ZO. As such, SCC tends to occur embedded into a cyclonic WR life cycle and often manifests within a ZO life cycle. This is also in agreement with the sharp increase in ZO frequency already prior to the SCC onset (Figures 2c and 2d). If anticyclonic regimes are associated with SCC at 65°N, these life cycles also start before the occurrence of SCC but there is a tendency for them to end during SCC (Figure 3a). When SCC occurs at 55°N, the prevailing associated cyclonic WR life cycles build up before the SCC onset and end after the SCC period (Figure 3b). Thus, a very similar behavior of the cyclonic regimes can be seen here as for SCC at 65°N. In contrast to SCC at 65°N, AT dominates the share of WR life cycles during SCC at 55°N and also shows the strongest tendency for SCC periods to manifest within a regime. Again, anticyclonic WR life cycles all start prior to SCC onset and show a tendency to decay before the SCC period ends. In contrast to SCC at 55°N and 65°N, the anticyclonic GL dominates the large-scale circulation around SCC periods at 45°N (Figure 3c). GL life cycles usually start before the occurrence of SCC, and—compared to the cyclonic regime life cycles associated with SCC in mid and high latitudes—start also much earlier in time. Other anticyclonic WR life cycles mostly build up before SCC onset and—including GL—to degrade after SCC decay. Interestingly, for SCC at 45°N cyclonic WR life cycles (in particular the few ZO, ScTr WR life cycles) tend to decay during SCC similar to the few anticyclonic WR life cycles for SCC at 55°N and 65°N.

Regardless of the selected latitude, most WR life cycles associated with SCC build up prior to and decay after the SCC period. Thus, we conclude that SCC periods typically occur within WR life cycles (Figure 3). However, few anticyclonic WR life cycles connected with SCC at 65°N and 55°N tend to decay within the SCC period. Overall, we cannot state if the WR or SCC is the cause for the other, but this investigation shows that SCC is strongly interlinked with WR life cycles.

4. Summary and Conclusions

We have found a close relationship between SCC at three latitudes (65°N, 55°N, and 45°N) in Western Europe and WRs for the NAE based on 40 winter periods (1979–2019). This relationship differs depending on the location. While for mid and high latitudes (55°N, 65°N) SCC is often associated with an increase in frequency of cyclonic WRs, SCC in low latitudes (45°N) is often linked with anticyclonic WRs, primarily GL but also sometimes the cyclonic AT WR. Regarding the question whether SCC precedes the associated WR or whether the WR sets in before SCC occurs, we have found a strong indication that WR life cycles build up before SCC and also outlast the SCC period. Exceptions are the anticyclonic WR life cycles associated with SCC in mid and high latitudes, which can degrade already during the SCC period.

Our novel results shed light on the mutual linkage of the general variability of the large-scale extra-tropical circulation as depicted by WRs and the compound extreme constituted by SCC events affecting a particular

region (Dacre & Pinto, 2020; Pinto et al., 2014). It corroborates the findings by Priestley et al. (2017a) that SCC at different latitudes in Europe go along with marked differences in the large-scale flow pattern. Given that WRs are expected to be more predictable at S2S time scales than individual cyclones (Büeler et al., 2021; Hannachi et al., 2017; Matsueda & Palmer, 2018), the new insight presented here may facilitate a better estimation on the probability of occurrence of storm series and associated impacts for time scales beyond 2 weeks, which are outside the current forecast skill horizon (e.g., Befort et al., 2019). In particular, slower modes of the climate system might provide predictability for regimes on S2S time scales. In winter, the stratospheric polar vortex substantially modulates the occurrence of WRs (Beerli & Grams, 2019). On the one hand, cyclonic ZO and ScTr regimes are more prevalent during a strong stratospheric polar vortex, while on the other hand anticyclonic GL and the AT regime are more prevalent during weak stratospheric polar vortices, leading to concomitant wind extremes in different European sub-regions (Beerli & Grams, 2019). Indeed, the recent Central European SCC period in February 2022 was embedded in a cyclonic regime preceded by an extremely strong stratospheric polar vortex (NASA Ozone Watch, 2022). Thus, not only regimes, but also slower climate modes might be important precursors to SCC. The linkage of SCC to modulations by the winter stratospheric polar vortex is subject of our ongoing research. This study has only considered specific cyclone tracking, clustering and WR methodologies, and focused exclusively on one longitude across Western Europe. Thus, the obtained relationships may be different if other methodologies, thresholds, and regions are considered. Therefore, further investigations on this topic will be key to derive robust assessments on the relationship between the large-scale circulation and the occurrence of cyclone clustering.

Nomenclature

AR	Atlantic Ridge
AT	Atlantic Trough
ECMWF	European Centre for Medium-Range Weather Forecasts
EuBL	European Blocking
GL	Greenland Blocking
NAE	North Atlantic-European region (80°W–40°E, 30°N–90°N)
NAO	North Atlantic Oscillation
ScBL	Scandinavian Blocking
SCC	Serial cyclone clustering
ScTr	Scandinavian Trough
S2S	Sub-seasonal to seasonal
WR	Weather regime
ZO	Zonal regime

Data Availability Statement

The results presented in this manuscript were created exclusively based on ERA-Interim reanalysis data (Dee et al., 2011) from the European Centre for Medium-Range Weather Forecasts (ECMWF). The data are available on the official ECMWF webpage (https://www.ecmwf.int/en/forecasts/datasets/reanalysis-datasets/era-interim; accessed 27 May 2022). The methods used to determine weather regimes and serial cyclone clustering periods are thoroughly described in detail and referenced in Section 2. Figures were made with Python version 3.7.4—available at https://www.python.org/—and maps were created through the cartopy python package.

Acknowledgments
The research leading to these results was partly embedded within the subprojects A8 "Dynamics and predictability of blocked regimes in the Atlantic-European region" and C8 "Stratospheric influence on predictability of persistent weather patterns" of the Transregional Collaborative Research Center SFB/TRR 165 "Waves to Weather" (www.wavestoweather.de) funded by the German Research Foundation (DFG). JGP thanks the AXA Research Fund for support. The contribution of CMG is funded by the Helmholtz Association as part of the Young Investigator Group "Sub-seasonal Predictability: Understanding the Role of Diabatic Outflow" (SPREADOUT, Grant VH-NG-1243). TCC was funded by BMBF ClimXtreme—Modul A "Physics and Processes," A6 Cyclex: Intensity and structural changes of extreme mid-latitude cyclones change in a warming climate (Grant 01LP1901A). We thank Matthew Priestley (University of Exeter) for help with the cyclone tracking data and acknowledge the Deutscher Wetterdienst and ECMWF for providing access to ECMWF data. Open Access funding enabled and organized by Projekt DEAL.

References

Beerli, R., & Grams, C. M. (2019). Stratospheric modulation of the large-scale circulation in the Atlantic–European region and its implications for surface weather events. *Quarterly Journal of the Royal Meteorological Society*, *145*(725), 3732–3750. https://doi.org/10.1002/qj.3653

Befort, D. J., Wild, S., Knight, J. R., Lockwood, J. F., Thornton, H. E., Hermanson, L., et al. (2019). Seasonal forecast skill for extratropical cyclones and windstorms. *Quarterly Journal of the Royal Meteorological Society*, *145*(718), 92–104. https://doi.org/10.1002/qj.3406

Bevacqua, E., De Michele, C., Manning, C., Couasnon, A., Ribeiro, A. F. S., Ramos, A. M., et al. (2021). Guidelines for studying diverse types of compound weather and climate events. *Earth's Future*, *9*(11), e2021EF002340. https://doi.org/10.1029/2021EF002340

Bjerknes, J., & Solberg, H. (1922). Life cycle of cyclones and the polar front theory of atmospheric circulation. *Geofysiske Publikasjoner*, *3*(1), 3–18.

Büeler, D., Ferranti, L., Magnusson, L., Quinting, J. F., & Grams, C. M. (2021). Year-round sub-seasonal forecast skill for Atlantic–European weather regimes. *Quarterly Journal of the Royal Meteorological Society*, *147*(741), 4283–4309. https://doi.org/10.1002/qj.4178

Cattiaux, J., Vautard, R., Cassou, C., Yiou, P., Masson-Delmotte, V., & Codron, F. (2010). Winter 2010 in Europe: A cold extreme in a warming climate. *Geophysical Research Letters*, *37*(20), L20704. https://doi.org/10.1029/2010GL044613

Charney, J. G., & DeVore, J. G. (1979). Multiple flow equilibria in the atmosphere and blocking. *Journal of the Atmospheric Sciences*, *36*(7), 1205–1216. https://doi.org/10.1175/1520-0469

Dacre, H. F., & Pinto, J. G. (2020). Serial clustering of extratropical cyclones: A review of where, when and why it occurs. *NPJ Climate and Atmospheric Science*, *3*(48), 48. https://doi.org/10.1038/s41612-020-00152-9

Dangendorf, S., Arns, A., Pinto, J. G., Ludwig, P., & Jensen, J. (2016). The exceptional influence of storm 'Xaver' on design water levels in the German bight. *Environmental Research Letters*, *11*(5), 054001. https://doi.org/10.1088/1748-9326/11/5/054001

Dee, D. P., Uppala, S. M., Simmons, A., Berrisford, P., Poli, P., Kobayashi, S., et al. (2011). The era-interim reanalysis: Configuration and performance of the data assimilation system. *Quarterly Journal of the Royal Meteorological Society*, *137*(656), 553–597. https://doi.org/10.1002/qj.828

Domeisen, D. I. V., Grams, C. M., & Papritz, L. (2020). The role of north Atlantic–European weather regimes in the surface impact of sudden stratospheric warming events. *Weather and Climate Dynamics*, *1*(2), 373–388. https://doi.org/10.5194/wcd-1-373-2020

Dunstone, N., Scaife, A. A., MacLachlan, C., Knight, J., Ineson, S., Smith, D., et al. (2018). Predictability of European winter 2016/2017. *Atmospheric Science Letters*, *19*(12), e868. https://doi.org/10.1002/asl.868

Falkena, S. K., de Wiljes, J., Weisheimer, A., & Shepherd, T. G. (2020). Revisiting the identification of wintertime atmospheric circulation regimes in the euro-Atlantic sector. *Quarterly Journal of the Royal Meteorological Society*, *146*(731), 2801–2814. https://doi.org/10.1002/qj.3818

Faranda, D., Masato, G., Moloney, N., Sato, Y., Daviaud, F., Dubrulle, B., & Yiou, P. (2016). The switching between zonal and blocked mid-latitude atmospheric circulation: A dynamical system perspective. *Climate Dynamics*, *47*(5), 1587–1599. https://doi.org/10.1007/s00382-015-2921-6

Faranda, D., Messori, G., & Yiou, P. (2017). Dynamical proxies of north Atlantic predictability and extremes. *Scientific Reports*, *7*(1), 41278. https://doi.org/10.1038/srep41278

Fink, A. H., Brücher, T., Ermert, V., Krüger, A., & Pinto, J. G. (2009). The European storm Kyrill in January 2007: Synoptic evolution, meteorological impacts and some considerations with respect to climate change. *Natural Hazards and Earth System Sciences*, *9*(2), 405–423. https://doi.org/10.5194/nhess-9-405-2009

Grams, C. M., Beerli, R., Pfenninger, S., Staffell, I., & Wernli, H. (2017). Balancing Europe's wind-power output through spatial deployment informed by weather regimes. *Nature Climate Change*, *7*(8), 557–562. https://doi.org/10.1038/NCLIMATE3338

Hannachi, A., Straus, D. M., Franzke, C. L. E., Corti, S., & Woollings, T. (2017). Low-frequency nonlinearity and regime behavior in the northern hemisphere extratropical atmosphere. *Reviews of Geophysics*, *55*(1), 199–234. https://doi.org/10.1002/2015RG000509

Hochman, A., Messori, G., Quinting, J. F., Pinto, J. G., & Grams, C. M. (2021). Do Atlantic-European weather regimes physically exist? *Geophysical Research Letters*, *48*(20), e2021GL095574. https://doi.org/10.1029/2021GL095574

Lavaysse, C., Vogt, J., Toreti, A., Carrera, M. L., & Pappenberger, F. (2018). On the use of weather regimes to forecast meteorological drought over Europe. *Natural Hazards and Earth System Sciences*, *18*(12), 3297–3309. https://doi.org/10.5194/nhess-18-3297-2018

Levick, R. B. M. (1949). Fifty years of English weather. *Weather*, 4(7), 206–211. https://doi.org/10.1002/j.1477-8696.1949.tb05487.x

Mailier, P. J., Stephenson, D. B., Ferro, C. A. T., & Hodges, K. I. (2006). Serial clustering of extratropical cyclones. *Monthly Weather Review*, *134*(8), 2224–2240. https://doi.org/10.1175/MWR3160.1

Matsueda, M., & Palmer, T. N. (2018). Estimates of flow-dependent predictability of wintertime euro-Atlantic weather regimes in medium-range forecasts. *Quarterly Journal of the Royal Meteorological Society*, *144*(713), 1012–1027. https://doi.org/10.1002/qj.3265

Matthews, T., Murphy, C., Wilby, R. L., & Harrigan, S. (2014). Stormiest winter on record for Ireland and UK. *Nature Climate Change*, *4*(9), 738–740. https://doi.org/10.1038/nclimate2336

Merryfield, W. J., Baehr, J., Batté, L., Becker, E. J., Butler, A. H., Coelho, C. A. S., et al. (2020). Current and emerging developments in subseasonal to decadal prediction. *Bulletin of the American Meteorological Society*, *101*(6), E869–E896. https://doi.org/10.1175/BAMS-D-19-0037.1

Messori, G., & Caballero, R. (2015). On double Rossby wave breaking in the north Atlantic. *Journal of Geophysical Research: Atmospheres*, *120*(21), 11129–11150. https://doi.org/10.1002/2015JD023854

Michel, C., & Rivière, G. (2011). The link between Rossby wave breakings and weather regime transitions. *Journal of the Atmospheric Sciences*, *68*(8), 1730–1748. https://doi.org/10.1175/2011JAS3635.1

Mühr, B., Eisenstein, L., Pinto, J. G., Knippertz, P., Mohr, S., & Kunz, M. (2022). *Winter storm series: Ylenia, Zeynep, Antonia (int: Dudley, Eunice, Franklin) February 2022 (NW and Central Europe)*. Technical Report No. March 2022 (Vol. 1). CEDIM Forensic Disaster Analysis Group (FDA). https://doi.org/10.5445/IR/1000143470

Murray, R. J., & Simmonds, I. (1991). A numerical scheme for tracking cyclone centres from digital data. *Australian Meteorological Magazine*, *39*(3), 155–166.

NASA Ozone Watch. (2022). 60°N zonal mean zonal wind at 10 hPa (MERRA2). Retrieved from https://ozonewatch.gsfc.nasa.gov/meteorology/figures/merra2/wind/u60n_10_2021_merra2.pdf

Neu, U., Akperov, M. G., Bellenbaum, N., Benestad, R., Blender, R., Caballero, R., et al. (2013). IMILAST: A community effort to intercompare extratropical cyclone detection and tracking algorithms. *Bulletin of the American Meteorological Society*, *94*(4), 529–547. https://doi.org/10.1175/BAMS-D-11-00154.1

Osborn, T. J. (2011). Winter 2009/2010 temperatures and a record-breaking north Atlantic oscillation index. *Weather*, *66*(1), 19–21. https://doi.org/10.1002/wea.660

Parker, D. J. (1998). Secondary frontal waves in the north Atlantic region: A dynamical perspective of current ideas. *Quarterly Journal of the Royal Meteorological Society*, *124*(547), 829–856. https://doi.org/10.1002/qj.49712454709

Pasquier, J. T., Pfahl, S., & Grams, C. M. (2019). Modulation of atmospheric river occurrence and associated precipitation extremes in the North Atlantic region by European weather regimes. *Geophysical Research Letters*, *46*(2), 1014–1023. https://doi.org/10.1029/2018GL081194

Pinto, J. G., Gómara, I., Masato, G., Dacre, H. F., Woollings, T., & Caballero, R. (2014). Large-scale dynamics associated with clustering of extratropical cyclones affecting Western Europe. *Journal of Geophysical Research: Atmospheres*, *119*(22), 13704–13719. https://doi.org/10.1002/2014JD022305

Pinto, J. G., Spangehl, T., Ulbrich, U., & Speth, P. (2005). Sensitivities of a cyclone detection and tracking algorithm: Individual tracks and climatology. *Meteorologische Zeitschrift*, *14*(6), 823–838. https://doi.org/10.1127/0941-2948/2005/0068

Pinto, J. G., Zacharias, S., Fink, A. H., Leckebusch, G. C., & Ulbrich, U. (2009). Factors contributing to the development of extreme North Atlantic cyclones and their relationship with the NAO. *Climate Dynamics*, *32*(5), 711–737. https://doi.org/10.1007/s00382-008-0396-4

Priestley, M. D. K., Pinto, J. G., Dacre, H. F., & Shaffrey, L. C. (2017b). Rossby wave breaking, the upper level jet, and serial clustering of extratropical cyclones in western Europe. *Geophysical Research Letters*, *44*(1), 514–521. https://doi.org/10.1002/2016GL071277

Priestley, M. D. K., Pinto, J. G., Dacre, H. F., & Shaffrey, L. C. (2017a). The role of cyclone clustering during the stormy winter of 2013/2014. *Weather*, *72*(7), 187–192. https://doi.org/10.1002/wea.3025

Santos, J. A., Belo-Pereira, M., Fraga, H., & Pinto, J. G. (2016). Understanding climate change projections for precipitation over western Europe with a weather typing approach. *Journal of Geophysical Research: Atmospheres*, *121*(3), 1170–1189. https://doi.org/10.1002/2015JD024399

Vitolo, R., Stephenson, D. B., Cook, I. M., & Mitchell-Wallace, K. (2009). Serial clustering of intense European storms. *Meteorologische Zeitschrift*, *18*(4), 411–424. https://doi.org/10.1127/0941-2948/2009/0393

Wanner, H., Brönnimann, S., Casty, C., Gyalistras, D., Luterbacher, J., Schmutz, C., et al. (2001). North Atlantic oscillation—Concepts and studies. *Surveys in Geophysics*, *22*(4), 321–382. https://doi.org/10.1023/A:1014217317898

Weijenborg, C., & Spengler, T. (2020). Diabatic heating as a pathway for cyclone clustering encompassing the extreme storm Dagmar. *Geophysical Research Letters*, *47*(8), e2019GL085777. https://doi.org/10.1029/2019GL085777

White, C. J., Domeisen, D. I. V., Acharya, N., Adefisan, E. A., Anderson, M. L., Aura, S., et al. (2021). Advances in the application and utility of subseasonal-to-seasonal predictions. *Bulletin of the American Meteorological Society*, *1*(aop), 1–57. https://doi.org/10.1175/BAMS-D-20-0224.1

Yiou, P., & Nogaj, M. (2004). Extreme climatic events and weather regimes over the North Atlantic: When and where? *Geophysical Research Letters*, *31*(7), L07202. https://doi.org/10.1029/2003GL019119

Zscheischler, J., Martius, O., Westra, S., Bevacqua, E., Raymond, C., Horton, R. M., et al. (2020). A typology of compound weather and climate events. *Nature Reviews Earth & Environment*, *1*(1), 333–347. https://doi.org/10.1038/s43017-020-0060-z